ACCEPTED VERSION

Stuart T. Johnston, Joshua V. Ross, Benjamin J. Binder, D.L. Sean McElwain, Parvathi Haridas, Matthew J. Simpson
Quantifying the effect of experimental design choices for in vitro scratch assays
Journal of Theoretical Biology, 2016; 400:19-31

© 2016 Elsevier Ltd. All rights reserved.

This manuscript version is made available under the CC-BY-NC-ND 4.0 license
http://creativecommons.org/licenses/by-nc-nd/4.0/

Final publication at http://dx.doi.org/10.1016/j.jtbi.2016.04.012

PERMISSIONS

https://www.elsevier.com/about/our-business/policies/sharing

Accepted Manuscript

Authors can share their accepted manuscript:

[12 months embargo]

After the embargo period

- via non-commercial hosting platforms such as their institutional repository
- via commercial sites with which Elsevier has an agreement

In all cases accepted manuscripts should:

- link to the formal publication via its DOI
- bear a CC-BY-NC-ND license – this is easy to do
- if aggregated with other manuscripts, for example in a repository or other site, be shared in alignment with our hosting policy
- not be added to or enhanced in any way to appear more like, or to substitute for, the published journal article

24 June 2020

http://hdl.handle.net/2440/101599

Quantifying the effect of experimental design choices for *in vitro* scratch assays

Stuart T. Johnston[a,b], Joshua V. Ross[c], Benjamin J. Binder[c], DL. Sean McElwain[a,b], Parvathi Haridas[b], Matthew J. Simpson[a,b,*]

[a] *School of Mathematical Sciences, Queensland University of Technology (QUT), Brisbane, Australia.*
[b] *Institute of Health and Biomedical Innovation, QUT, Brisbane, Australia.*
[c] *School of Mathematical Sciences, University of Adelaide, Adelaide, Australia.*

Abstract

Scratch assays are often used to investigate potential drug treatments for chronic wounds and cancer. Interpreting these experiments with a mathematical model allows us to estimate the cell diffusivity, D, and the cell proliferation rate, λ. However, the influence of the experimental design on the estimates of D and λ is unclear. Here we apply an approximate Bayesian computation (ABC) parameter inference method, which produces a posterior distribution of D and λ, to new sets of synthetic data, generated from an idealised mathematical model, and experimental data for a non-adhesive mesenchymal population of fibroblast cells. The posterior distribution allows us to quantify the amount of information obtained about D and λ. We investigate two types of scratch assay, as well as varying the number and timing of the experimental observations captured. Our results show that a scrape assay, involving one cell front, provides more precise estimates of D and λ, and is more computationally efficient to interpret than a wound assay, with two opposingly-directed cell fronts. We find that recording two observations, after making the initial observation, is sufficient to estimate D and λ, and that the final observation time should correspond to the time taken for the cell front to move across the field of view. These results provide guidance for estimating D and λ, while simultaneously minimising the time and cost associated with performing and interpreting the experiment.

Keywords: Scratch assay, Experimental design, Approximate Bayesian computation, Cell motility, Cell proliferation

1. Introduction

Scratch assays are commonly used to observe the migration and proliferation of cells [11, 19, 20, 21, 27, 41]. Cells are placed on a culture dish and incubated, eventually forming a confluent monolayer [21]. An artificial

*Corresponding author
Email address: matthew.simpson@qut.edu.au (Matthew J. Simpson)

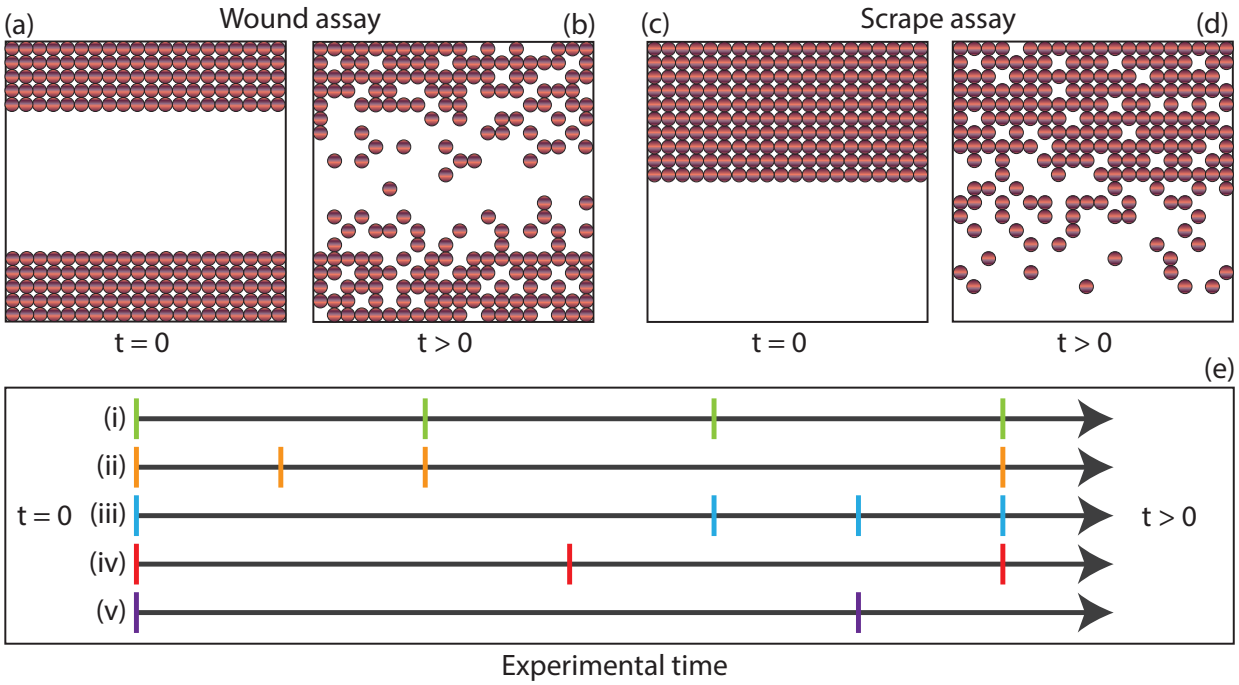

Figure 1: Schematic representation of scratch assay design parameters. (a)-(b) Schematic wound assay. (a) Immediately after the scratch, and (b) as the two fronts move and the wound begins to close. (c)-(d) Schematic scrape assay. (c) Immediately after the scratch, and (d) as the single cell front moves. (e) Potential combinations of the timing of experimental observations.

wound is created and images of the resulting collective cell spreading, driven by combined cell migration and proliferation, are captured over 12-24 hours [1, 5, 25, 26, 30]. The number of experimental images captured and reported varies considerably. For example, some results that are reported include just one or two observations [1, 26, 30], whereas others report many more [5, 14, 25]. The influence of the number of observations on the experimental findings has not been quantified.

The majority of scratch assays fall into one of two categories. The first, which we refer to as a *wound assay*, involves the creation of a thin wound [21, 27], which produces two opposingly directed cell fronts that eventually merge [1], as shown in the schematic in Figures 1(a)-(b). The second, which we refer to as a *scrape assay*, involves a monolayer that has been more extensively scratched so there is only one cell front [5, 23], as shown in the schematic in Figures 1(c)-(d). Again, the influence of the assay choice on the experimental findings has not been quantified.

Previously, scratch assays have been used to investigate the influence of various chemical compounds and potential drug treatments on the rates of cell motility and proliferation [11, 19, 20, 41]. For example, wound healing can be stimulated by steroid treatment [41], while cell proliferation can be inhibited by

chemotherapeutic drugs [29]. Developing methods that allow us to robustly quantify the rates of cell migration and proliferation is therefore critical to drug design. However, the majority of scratch assay results are interpreted qualitatively [20, 26] or use simple quantitative measures that do not distinguish between the roles of cell motility and proliferation [11, 19]. In contrast, mathematical models that explicitly distinguish between the roles of cell diffusivity, D, and cell proliferation, λ, for scratch assays have also been presented [5, 12, 14, 15, 16, 17, 28, 40]. Previous approaches using both deterministic models [14, 15] and stochastic models [16] lead to point-estimates of D and λ. More recently, approximate Bayesian computation (ABC) has been used to provide estimates of D and λ, together with a measure of the uncertainty associated with these estimates [17]. While ABC methods are computationally demanding compared to deterministic data calibration techniques, such as the Levenberg-Marquadt algorithm [15], the advantage of ABC is that additional information regarding the uncertainty of the model parameter estimates is obtained. Furthermore, prior knowledge about the system can be incorporated in a principled and systematic way, such that knowledge can be accumulated as more data is available. The ABC method of Johnston and coworkers [17] has been used to obtain parameter estimates for 3T3 fibroblasts but did not consider the influence of design parameters on the model parameter estimates.

In this work we refer to two different categories of parameters:

- *Model parameters*, which govern the cell diffusivity, D, and cell proliferation rate, λ, and
- *Design parameters*, which distinguish between different experimental designs of a scratch assay, such as shown in Figure 1.

It is instructive to consider how the posterior distribution of D and λ from the ABC algorithm is influenced by the choice of design parameters. The information gained in moving from a prior to a posterior distribution can be quantified using the Kullback-Leibler divergence, D_{KL} [4]. Numerical approximations of posterior distributions are calculated using ABC [24] and have been applied to parameter inference in dynamical systems [37] and spatio-temporal models [17, 42]. Bayesian experimental design is concerned with determining the optimal experimental design that maximises D_{KL}, by adjusting the design parameters [6]. Our mathematical framework, which mimics the random motility and proliferation of mesenchymal (non-adhesive) cells in a scratch assay, contains a significant number of design parameters [17, 32]. However, we require that the design parameters can be adjusted experimentally, as well as in the mathematical model, otherwise the results may have limited practical relevance. The simplest design parameter to alter is the number and timing of the experimental observations. An example of different combinations of experimental observations is presented in Figure 1(e). The combination of observation times in (i) contains four equally-spaced observations, whereas in (ii) and (iii) the observations are clustered at the start and end of the experiment, respectively. Currently, it is unclear which combination of observation times provides

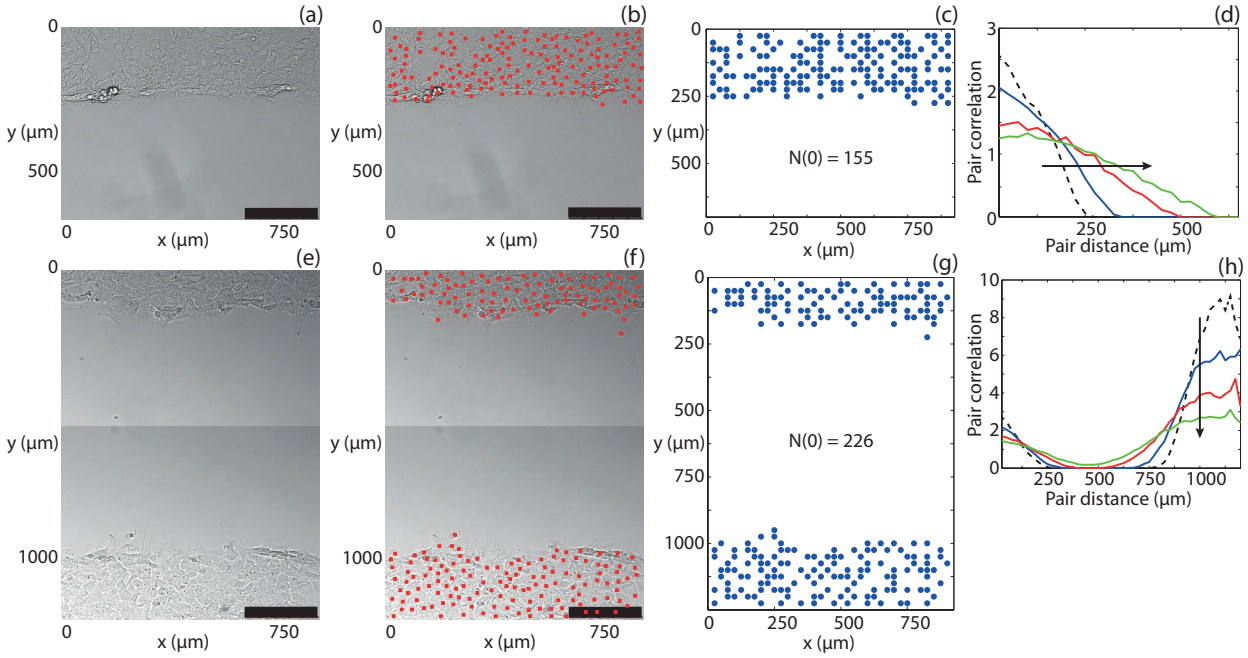

Figure 2: Interpretation of experimental images for (a)-(d) the scrape assay and (e)-(h) the wound assay. (a),(e) Experimental images. (b),(f) Identification of the position of cells. The red markers denote the cell centres, and the markers are deliberately chosen to be smaller than the size of the individual cells so that individual cells are not obscured. The scale bar corresponds to 300 μm. (c),(g) Cell positions mapped to a square lattice with $\Delta = 25$ μm. (d),(h) Temporal evolution of the pair correlation function. The pair correlation function is presented at 0 h (dashed black), 4 h (blue), 8 h(red) and 12 h (green). The arrows indicate the direction of increasing time.

the most information about the model parameters, D and λ, and Bayesian experimental design allows us to quantify these differences. Therefore, we may be able to identify the optimal number of experimental images required and consequently avoid collecting additional unnecessary observations, reducing the cost associated with performing and interpreting the experiments.

Here we implement the ABC parameter inference method of Johnston and coworkers [17]. In Section 2 we provide a brief description of the experimental procedure and the mathematical model. The influence of the assay choice on the model parameter estimates, using both synthetic and experimental data sets, is examined in Section 3. We also investigate the influence of the number and timing of observations on the model parameter estimates, using both synthetic and experimental data sets. In Section 4 we discuss the implications of our results, and in Section 5, we make recommendations about the experimental design, and suggest options for future work.

2. Methods

2.1. Experimental method

The experimental method has been presented previously [34]. Briefly, murine fibroblast 3T3 cells [36] are grown in T175 cm^2 tissue culture flasks and one μL of cell suspension is placed into the well of a tissue culture plate. The tissue culture plate is incubated at 37 °C in 5% CO_2 overnight so that the cell population settles, attaches to the substrate, and the density begins to increase as cell proliferation takes place. A scratch is made in the monolayer using a P100 pipette tip for the wound assay, and a P1000 pipette tip for the scrape assay. Microscopic images are captured every five minutes for 24 hours after the initial scratch is made using a Leica AF6000 automated microscope. Experimental images of the scrape and wound assays are given in Figures 2(a) and (e), respectively. We note that the cell populations in Figures 2(a) and (e) appear to be confluent away from the scratched region. However, 3T3 fibroblasts are known to grow to reach significantly higher densities than in Figures 2(a) and (e) [34]. This implies that the cell density will increase well beyond the density in Figures 2(a) and (e) provided that sufficient time is allowed for more cell proliferation to take place.

2.2. Mathematical model

Individual-based random walk models with crowding effects are widely used to mimic the behaviour of cells in biological systems [9, 16, 17, 22, 32]. We consider a two-dimensional random walk on a square lattice, with lattice spacing Δ [7, 32], where each site may be occupied by, at most, one agent. Agents have the potential to move and proliferate with constant probability $P_m \in [0, 1]$ and $P_p \in [0, 1]$, respectively, during each timestep of fixed duration τ. These probabilities are related to the diffusivity and proliferation rate by [32]

$$D = \frac{P_m \Delta^2}{4\tau}, \qquad \lambda = \frac{P_p}{\tau}. \tag{1}$$

Using these relationships we consider the parameters in the discrete model, (P_m, P_p, Δ, τ), as being interchangeable with the model parameters, D and λ [16, 17]. We treat Δ and τ as constants: Δ is measurable [34] and τ is a constant that is chosen to be sufficiently small that the results are independent of the time step [38]. For all simulations $\tau = 1/24$ h. Although our model is an exclusion process, whereby individual agents are subject to crowding effects, previous analysis has shown that the two-dimensional spreading of a population of these agents due to random motility with crowding is described by a linear diffusion mechanism with $D = P_m \Delta^2 / 4\tau$ [31].

In any simulation we have $N(t)$ agents, and during each timestep, $N(t)$ agents are selected sequentially at random, with replacement, and given the opportunity to move with probability P_m. If an agent undergoing a movement event is currently at (x, y) it attempts to move to $(x \pm \Delta, y)$ or $(x, y \pm \Delta)$, without bias. After $N(t)$ agents have attempted to move, an additional $N(t)$ agents are selected sequentially at random,

with replacement, and given the opportunity to proliferate with probability P_p. An agent undergoing a proliferation event at (x, y) will attempt to place a daughter agent at $(x \pm \Delta, y)$ or $(x, y \pm \Delta)$, without bias. Potential motility or proliferation events only succeed if the target site is vacant [32].

The geometry of a scratch assay is approximated with a lattice of height $Y\Delta$ and width $X\Delta$. The field of view of our microscope and average cell size provide a natural choice for Δ, Y and X. The average cell diameter of 3T3 fibroblasts has been measured previously, giving $\Delta = 25$ μm [34]. For our synthetic data set we consider an idealised case where X and Y are the same for both assays. For our experimental data set, the experimental image of a scrape assay in Figure 2(a) gives $Y = 27$ and $X = 36$, while the experimental image of a wound assay in Figure 2(e) gives $Y = 49$ and $X = 36$. Since the approximately spatially uniform population extends well beyond the boundaries of the field of view, there will be no net flux of cells across these boundaries [15]. Hence we apply no net flux (symmetry) boundary conditions along the lines $y = 0,\ y = Y\Delta,\ x = 0,\ x = X\Delta$ [15, 16, 17]. To model a scrape assay, we randomly place $N(0)$ agents in the region $y \leq Y_0\Delta$ such that each lattice site is occupied by, at most, one agent. We note that Y_0 is the height of the initially-occupied region in a scrape assay. Our wound assay contains a total of $N(0)$ agents in two regions, $y \leq Y_{0,1}\Delta$ and $y > (Y - Y_{0,2})\Delta$, where $Y_{0,1}$ and $Y_{0,2}$ are the height of the initially occupied regions at $y = 0$ and $y = Y\Delta$, respectively. To calculate $N(0)$ we count the number of cells in the relevant experimental observation at $t = 0$ h.

In the mathematical model we can alter X, Y, $N(0)$, the height of the initially-confluent monolayer and the number and timing of observations captured. However, since we aim to mimic an experiment, we recognise that some design parameters are constrained by the experimental procedure. For example, X and Y are defined by the field of view of the microscope. Therefore, without additional equipment, we cannot alter this feature of the experimental domain. In addition, $N(0)$ is determined by the cell density at confluence, which is cell-type specific and cannot be easily varied. The height of the initially confluent monolayer, either Y_0 or $Y_{0,1}$ and $Y_{0,2}$, depends on the instrument used to perform the scratch and is difficult to reproduce reliably, and is therefore inappropriate to consider as a design parameter. We therefore focus on varying the number and timing of experimental observations captured. A single observation must be captured to determine the state of the system at $t = 0$ h and, consequently, we can only vary the number of observations captured after the initial observation. Therefore, the number of experimental observations captured refers to the number of observations captured after the initial observation.

2.3. Data interpretation

Both the synthetic data set, produced by our mathematical model, and the experimental data set contain the spatial positions of $N(t)$ cells in each observation. We note that the cell positions in the experimental

data set are obtained manually while the cell positions in the synthetic data set are obtained automatically. However, it is computationally intractable to compare the data sets using the spatial position of all cells. Johnston and coworkers [17] found that considering the number of cells, $N(t)$, and the pair correlation function, $q(i)$ [3], provides a summary statistic that contains a large percentage of the complete information. A summary statistic provides a lower-dimensional summary of a data set that allows tractable comparisons between data sets [10, 24]. Full details of the pair correlation function are presented elsewhere [3], and are summarised here. Briefly, we count the number of pairs of cells, separated by a distance of $i\Delta$ μm, in the y-direction and define this as $c(i)$, which is the counts of pair distances. We note that we could repeat this for the x-direction, however since the initial distribution of cells in the x-direction is, on average, uniform, and remains uniform throughout the experiment [3], we choose to focus on the counts of pair distances in the y direction only. The counts of pair distances are normalised to obtain the pair correlation function

$$q(i) = \frac{c(i)}{X^2(Y-i)\rho\bar{\rho}}, \tag{2}$$

where $\rho = N(t)/(XY)$ is the mean density and $\bar{\rho} = (N(t)-1)/(XY-1)$. The process of obtaining $q(i)$ from the experimental images is shown in Figure 2. To do this we identify the position of the centre of each cell in Figures 2(a) and (e) and mark their position with a red square in Figures 2(b) and (f), respectively. The red markers are deliberately chosen to be smaller than the cell diameter so that superimposing the markers on the experimental images does not obscure the view of the cells. We map the cell positions onto the lattice described in Section 2.2. We present the resulting lattice for the cell positions identified in Figures 2(b) and (f) in Figures 2(c) and (g), respectively. The corresponding pair correlation functions are presented in Figures 2(d) and (h), respectively, at 0, 4, 8 and 12 h.

2.4. Approximate Bayesian computation

To investigate which values of D and λ can generate summary statistics that are consistent with our synthetic or experimental data set we apply an ABC algorithm [2, 17, 24, 35, 37]. The ABC algorithm involves performing M identically-prepared stochastic realisations of the mathematical framework described in Section 2.2 and uses a combination of $N(t)$ and $q(i)$ as a summary statistic to determine an approximate posterior distribution of D and λ [17]. We note that we consider the uniform prior distribution for all data sets. Further details are given in the Supplementary Material.

3. Results

3.1. Assay choice: synthetic data set

In the experimental literature there has been no explicit discussion of whether the choice of performing a scrape or wound assay influences our ability to estimate D and λ. Therefore, we attempt to recover estimates of D and λ from synthetic data sets generated from the mathematical framework, for both assays.

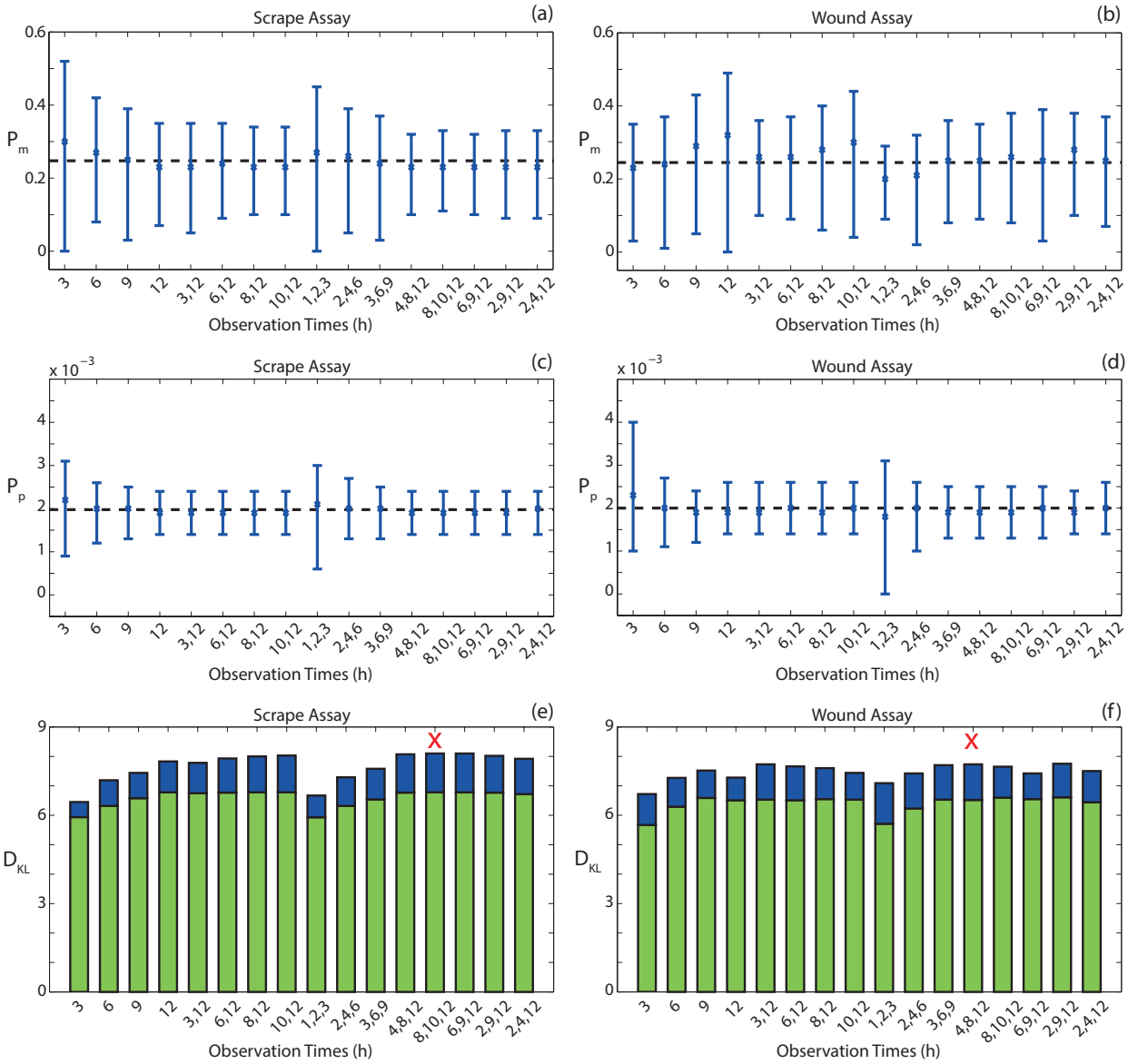

Figure 3: Mean model parameter estimates with 90% credible intervals, for a synthetically generated data set interpreted with a suite of combinations of observation times. (a)-(b) Mean estimates of P_m. (c)-(d) Mean estimates of P_p. The dashed line corresponds to the model parameter values used to obtain the synthetic data set. The blue crosses correspond to the mean values. (e)-(f) Mean D_{KL} values. The blue bar corresponds to the information gained about P_m and the green bar corresponds to information gained about P_p. The red crosses denote the combination of observation times that results in the highest D_{KL} value. Data was generated using $(P_m, P_p) = (0.25,\ 2 \times 10^{-3})$. For all simulations $\tau = 1/24$ h, $N(0) = 100$, $M = 10^6$, $X = 36$, $Y = 27$, $\Delta = 25$ μm. For scrape assays, $Y_0 = 10$. For wound assays, $Y_{0,1} = Y_{0,2} = 5$.

Observation Times (h)	3	6	9	12	3,12	6,12	8,12	10,12
Scrape Assay P_m 90% CI	0.52	**0.34**	**0.36**	**0.28**	0.30	**0.26**	**0.24**	**0.24**
Wound Assay P_m 90% CI	**0.32**	0.36	0.38	0.49	**0.26**	0.28	0.34	0.40
Scrape Assay P_p 90% CI (10^{-3})	**2.2**	**1.4**	**1.2**	**1.0**	**1.0**	**1.0**	**1.0**	**1.0**
Wound Assay P_p 90% CI (10^{-3})	3.0	1.6	**1.2**	1.2	1.2	1.2	1.2	1.2

Observation Times (h)	1,2,3	2,4,6	3, 6,9	4,8,12	8,10,12	6,9,12	2,9,12	2,4,12
Scrape Assay P_m 90% CI	0.45	0.34	0.34	**0.22**	**0.22**	**0.22**	**0.24**	**0.24**
Wound Assay P_m 90% CI	**0.20**	**0.30**	**0.28**	0.26	0.30	0.36	0.28	0.30
Scrape Assay P_p 90% CI (10^{-3})	**2.4**	**1.4**	**1.2**	**1.0**	**1.0**	**1.0**	**1.0**	**1.0**
Wound Assay P_p 90% CI (10^{-3})	3.1	1.6	**1.2**	1.2	1.2	1.2	**1.0**	1.2

Table 1: Comparison between the width of the 90% credible interval (CI), symmetric around the mode, for (i) P_m in the scrape assay; (ii) P_m in the wound assay; (iii) P_p in the scrape assay, and (iv) P_p in the wound assay for a suite of combinations of observation times. The assay type with the narrower credible interval for each combination of observation times and parameter is presented in bold.

We consider biologically relevant model parameters $(P_m, P_p) = (0.25, 2 \times 10^{-3})$, where cell proliferation occurs over a significantly longer timescale than cell motility [34]. We perform ten identically-prepared realisations of the mathematical model for both assays. For each realisation and assay we calculate $q(i)$ and $N(t)$ at $t = 0, 1, 2, ..., 12$ h [17]. We note that, in our synthetic experiments, $t = 12$ h approximately corresponds to the observed time taken for a cell front to move across a typical experimental field of view. For each realisation, we apply the ABC algorithm with the appropriate initial condition, and calculate the approximate posterior distribution of D and λ. For each assay, we then average the posterior distributions [16]. To measure the amount of information gained from the ABC algorithm we discretise the posterior distribution into 10^4 equally-spaced values of P_p, for $P_p \in [0, 1]$, and 10^2 equally-spaced values of P_m, for $P_m \in [0, 1]$. Since proliferation takes place on a longer timescale than motility [17, 39], we require a finer resolution for P_p than P_m. We then calculate the Kullback-Leibler divergence [4]

$$D_{KL}(f|\pi) = \sum_{j=1}^{10^6} f(\underline{\theta}_j|\beta) \ln\left(\frac{f(\underline{\theta}_j|\beta)}{\pi(\underline{\theta}_j)}\right), \tag{3}$$

where f is the posterior distribution, β is a data set, π is the uniform prior distribution, $\underline{\theta}$ is a model parameter pair and the index j accounts for all possible parameter pairs. We also calculate the marginal distributions for P_m and P_p by averaging the posterior distribution across P_p and P_m, respectively, and evaluate the corresponding value of D_{KL}. The mean and 90% credible interval, symmetrical around the mode, for P_m and P_p, are then estimated from the marginal distributions.

The posterior distributions of D and λ are calculated, for both assays, using a suite of combinations of observation times. Typically, scratch assays are interpreted with, at most, two observation times [1, 26, 30]. Therefore, we restrict our investigation to, at most, three observation times after the initial scratch is made.

The mean model parameter estimates and 90% credible intervals for both assays are given in Figures 3(a)-(d), indicating that the majority of combinations of observation times provide estimates of P_m and P_p that match those used to generate the synthetic data set for both assays. However, the credible intervals indicate that there is greater uncertainty in the estimates of P_m for the majority of combinations of observation times in the wound assay. We highlight the assay type with a narrower credible interval, corresponding to less uncertainty, for each combination of observation times in Figure 3 in Table 1. We attribute the greater uncertainty about P_m in the wound assay to the fact that the two cell fronts begin to interact toward the end of the experiment, which results in pair correlation functions that can be replicated with different values of P_m.

Interestingly, the credible intervals for P_p are similar for both the wound and scrape assay, suggesting that the difference in assay geometry does not influence the uncertainty associated with P_p. It is possible that the uncertainty associated with P_p is proportional to $N(0)$, which is the same for both synthetic assays. To explore this possibility, we repeat the synthetic scrape assay with $N(0) = 50$ and find that, for all combinations of observation times, there is more uncertainty in the recovered parameters compared to the synthetic scrape assay with $N(0) = 100$ (Tables 1-2, Supplementary Material). To examine the amount of information gained about the model parameters, we present D_{KL} for the suite of combinations of observation times, for both assay types, in Figures 3(e)-(f). Our results indicate that, predominantly, the scrape assay gives higher D_{KL} values when compared to the same combination of observation times in the wound assay. We note that there are cases where the D_{KL} value is higher for the wound assay. However, this occurs for combinations of observations times where the final observation is made at short time and hence these do not correspond to the designs that provide the most information. We denote the combination of observation times that provides the most information both the scrape and wound assay with a red cross in Figures 3(e)-(f), respectively. The most informative design in the scrape assay results in a D_{KL} value of 8.11, compared to 7.90 in the wound assay. For both assay types, the most informative design includes a final observation time at $t = 12$h, which corresponds to the final observation captured. We note that the Kullback-Leibler divergence is logarithmic, meaning that a large difference in uncertainty can correspond to a small difference in D_{KL}. To illustrate this, consider the D_{KL} values and uncertainty associated with P_p in the scrape assay at 1, 2, 3 h and 2, 4, 6 h. The D_{KL} values are 5.93 and 6.32, respectively, while the width of the 90% credible intervals are 2.4×10^{-3} and 1.4×10^{-3}, respectively. In this case a 6% increase in D_{KL} corresponds to a 42% reduction in the credible interval. Tabular form of the data in Figure 3 is provided in the Supplementary Material.

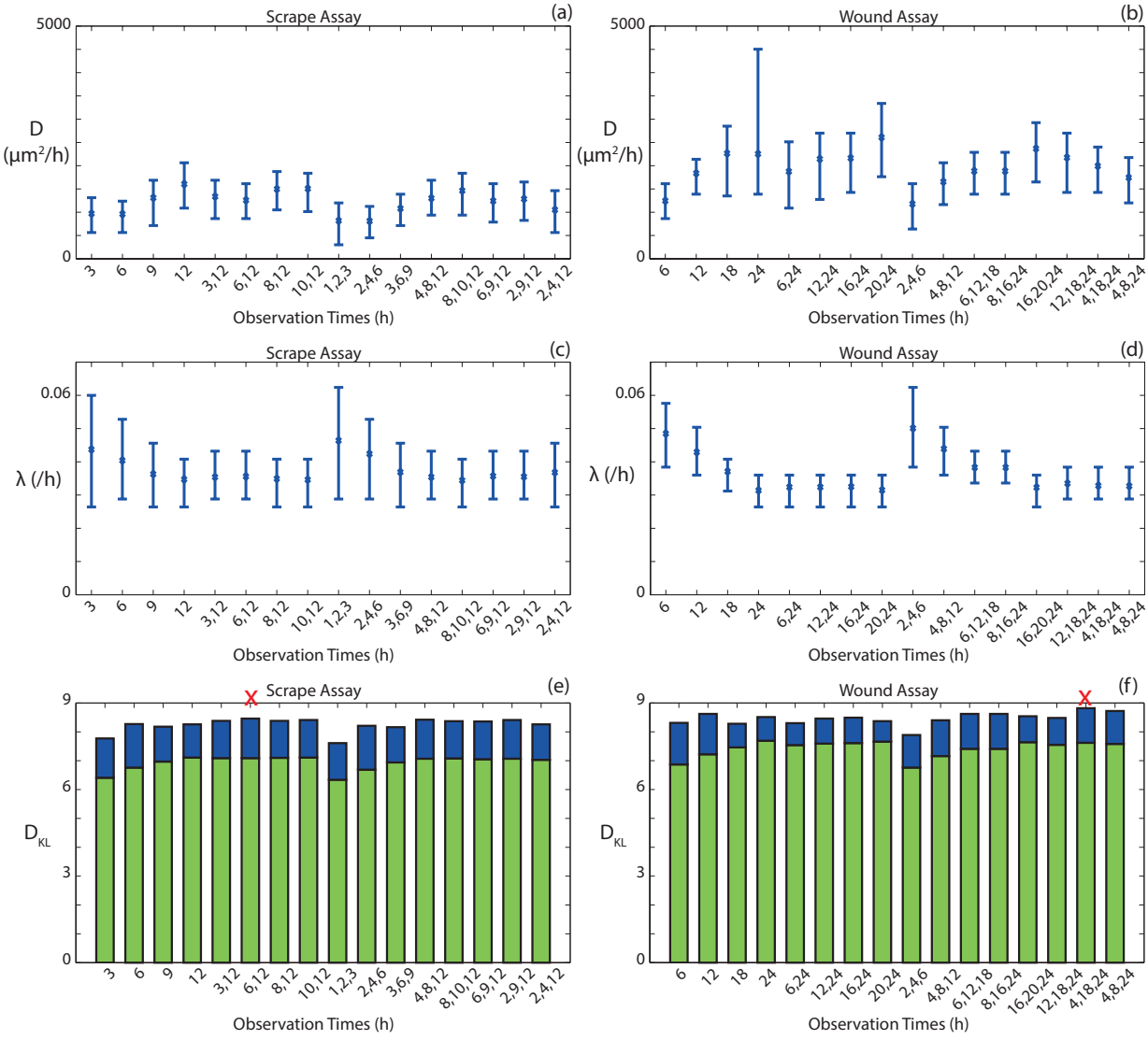

Figure 4: Mean model parameter estimates with 90% credible intervals, for an experimentally generated data set interpreted with a suite of combinations of observation times. (a)-(b) Mean estimates of D, given by Equation (3). (c)-(d) Mean estimates of λ. The blue crosses correspond to the mean values. (e)-(f) Mean D_{KL} values, given by Equation (3). The blue bar corresponds to the information gained about D and the green bar corresponds to information gained about λ. The red crosses denote the combination of observation times that results in the highest D_{KL} value. For all simulations $\tau = 1/24$ h, $M = 10^6$, $X = 36$, $Y = 27$, $\Delta = 25$ μm. For scrape assays, $N(0) = 155$, $Y_0 = 10$. For wound assays, $N(0) = 226$, $Y_{0,1} = 7$, $Y_{0,2} = 9$.

3.2. Assay choice: experimental data set

We now repeat the process in Section 3.1 for an experimental data set obtained using the procedure described in Section 2.1. We note that the wound assay was performed over 24 h whereas the scrape assay was performed over 12 h. These timescales were chosen since they indicate the amount of time required for the cell front(s) in the two different assays to move across their respective field of view. Without *a priori* information about D, it is difficult to choose an appropriate final time. Therefore, we capture experimental observations relatively frequently until the cell front has moved across the field of view. After the final observation has been captured, we select the relevant earlier observations to interpret our experimental results. While it is possible to capture experimental observations after the front(s) have moved across the field of view, it is unlikely that there is any additional information to be gained. Since the wound and scrape assays are different experiments, and hence are captured over different time periods, we compare combinations of observation times relative to the final time of the experiment, as this systematically utilises all relevant data for each experiment. For example, 6 and 12 h in the scrape assay are compared to 12 and 24 h in the wound assay. It would be computationally infeasible to explore all possible observation times and, as such, we attempt to provide a fair comparison by selecting observation times in a sensible manner.

We present mean estimates of D and λ, with 90% credible intervals, symmetric about the mode, for both assays in Figures 4(a)-(d). We observe that the qualitative trend for the mean model parameter estimates with regard to the combination of observation times is consistent for both assays. This suggests that comparing combinations of observation times after the same proportion of the final observation time is reasonable.

Unlike the synthetic data set, we observe that the scrape and wound assay provide different estimates of the cell diffusivity, D. Given that estimates of D for 3T3 fibroblasts are reported to be in the range 30-3000 $\mu\text{m}^2/\text{h}$ [5, 17, 39, 40], our observed variation is not necessarily surprising. However, we note that our estimates of D are consistent with previous results obtained by interpreting experiments using 3T3 cells with an ABC algorithm [17]. Comparing the credible intervals for the two assays we observe that, again, there is more uncertainty associated with D for the majority of combinations of observation times in the wound assay.

Our estimates of the cell proliferation rate, λ, from the two assays are similar. This is consistent with the synthetic data set, suggesting that estimates of λ are relatively insensitive to whether we consider a scrape or wound assay. However, the 90% credible intervals for λ are always smaller for the wound assay. The reduction in uncertainty may be attributed to the larger number of initial cells in the wound assay, as we observed similar credible intervals in the synthetic data set where $N(0)$ is the same for both assays. Evaluating the D_{KL} value for each combination of observation times and both assays, presented in Figures 4(e)-(f), respectively, suggests that more information is obtained from the wound assay. However, decom-

posing the D_{KL} value into the D_{KL} values for the marginal distributions for D and λ, which correspond to the blue and green bars in Figures 4(e)-(f), respectively, suggests that while more information is obtained about λ in the wound assay, the scrape assay provides more information about D. The most informative combination of observation times, denoted by the red crosses in Figures 4(e)-(f), provides more information in the wound assay than in the scrape assay. Again, however, this additional information is associated with λ. Furthermore, similar to the results obtained from the synthetic data set, the most informative combination of observations for both assays include the final experimental observation. Tabular form of the data in Figure 4 is provided in the Supplementary Material.

Unfortunately, the additional information obtained from the wound assay is associated with two important limitations. First, the interpretation of the experimental images is significantly more time-consuming due to higher $N(t)$ values. Second, the time required to perform the ABC algorithm for the experimental wound assay is significantly longer than for the experimental scrape assay, due to the increase in both the final time and initial number of cells. Running in parallel on ten cores (2.66 GHz Intel Xeon E5-2670), the ABC algorithm for the wound assay required approximately one week of computation time, whereas the scrape assay required approximately one day of computation time.

3.3. Choice of observation times: synthetic data set

Typically, in the experimental literature there is no explicit discussion about the choice of the duration of the experiment [1, 17, 19, 26]. Therefore, it is instructive to compare estimates of D and λ, and the corresponding D_{KL} values, for different final time points using synthetic data. Using the approximate posterior distributions generated in Section 3 we calculate the mean estimates of P_m and P_p, and the corresponding mean 90% credible intervals, symmetric around the mode, for a final observation time of 3, 6, 9 and 12 h. Results are presented in Figures 5(a)-(b) and Figures 5(d)-(e), for the scratch assay and the wound assay, respectively. For both assays we see that the mean parameter estimates depend on the choice of final observation time. To determine which final observation time provides the most information about D and λ we calculate the mean D_{KL} value, for both P_m and P_p, for each final observation time. The mean D_{KL} values are presented in Figures 5(c) and (f) for the scrape assay and wound assay, respectively. We note that the green bar reflects the information gained about P_p while the blue bar reflects the information gained about P_m. For the scrape assay, we observe that a final observation time of 12 h provides the most information about both P_m and P_p and note that 12 h corresponds to the approximate time taken for the cell front to move across the experimental field of view. This result is intuitive, as we are able to observe cell migration and proliferation until the cell front crosses, and leaves, the experimental field of view. For the wound assay, we observe that the information gained peaks at a final observation time of 9 h. Again, this result is intuitive as the two opposingly-directed cell fronts begin to interact towards the end of the experiment, and hence

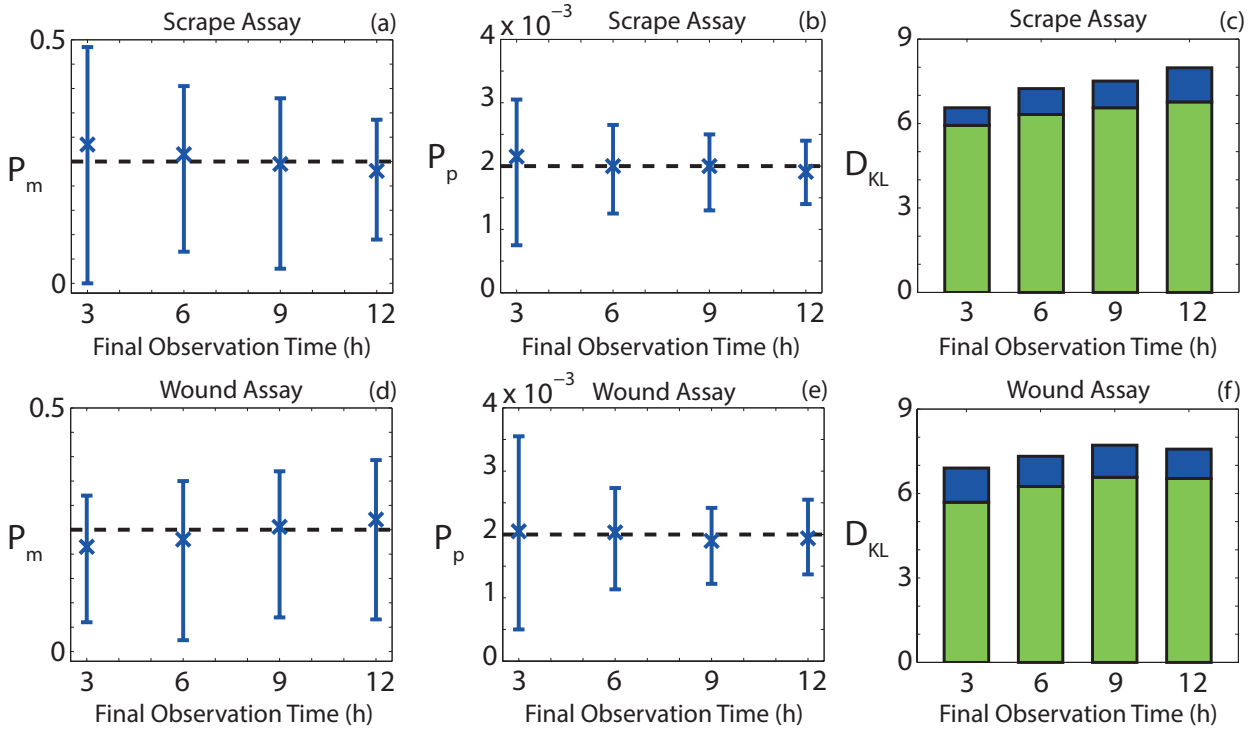

Figure 5: Results obtained from the parameter inference approach applied to the synthetic data set generated with $(P_m, P_p) = (0.25, 2 \times 10^{-3})$. (a)-(c) Mean estimates of P_m and P_p with corresponding 90% credible intervals, and the mean D_{KL} values, respectively, for the scrape assay for a final observation time of 3 h, 6 h, 9 h and 12 h. (d)-(f) Mean estimates of P_m and P_p with corresponding 90% credible intervals, and the mean D_{KL} values, respectively, for the wound assay for a final observation time of 3 h, 6 h, 9 h and 12 h. The mean D_{KL} values were calculated using Equation (3). The green bar corresponds to the D_{KL} value for P_p and the blue bar corresponds to the D_{KL} value for P_m. For all simulations $\tau = 1/24$ h, $N(0) = 100$, $M = 10^6$, $X = 36$, $Y = 27$, $\Delta = 25$ μm. For scrape assays, $Y_0 = 10$. For wound assays, $Y_{0,1} = Y_{0,2} = 5$. The crosses correspond to the mean values.

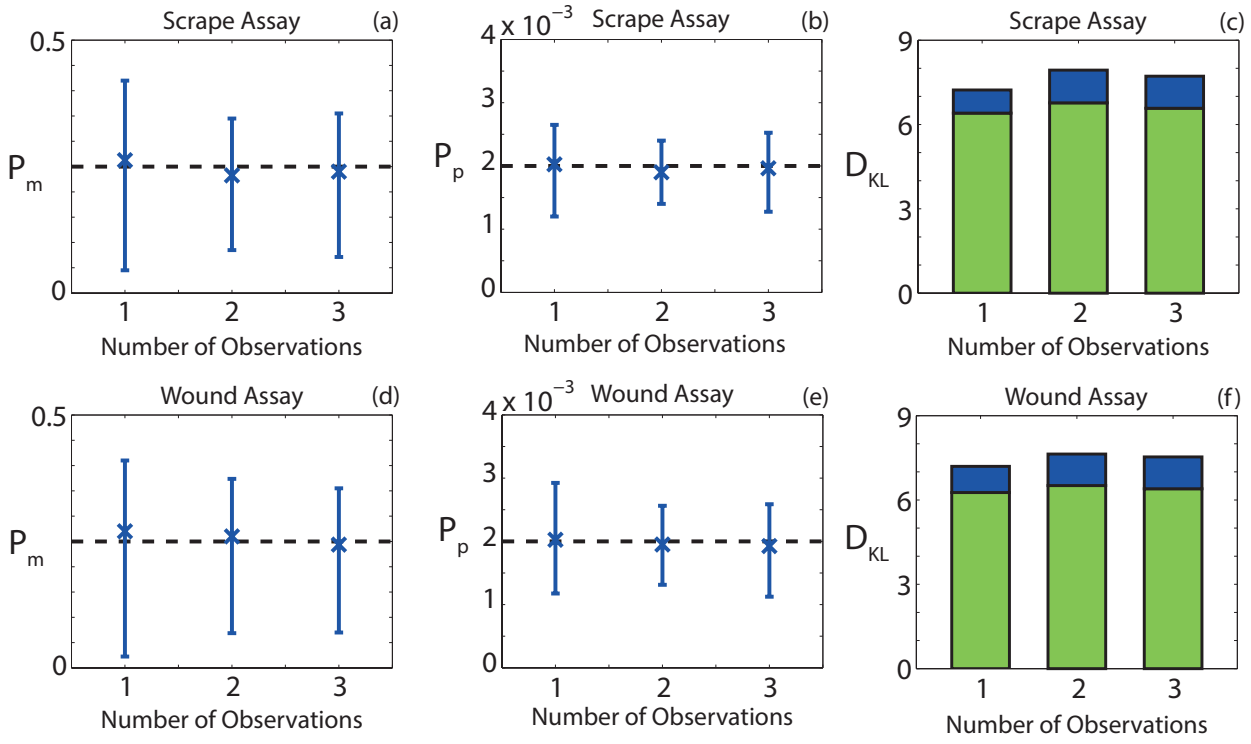

Figure 6: Results obtained from the parameter inference approach applied to the synthetic data set generated with $(P_m, P_p) = (0.25, 2 \times 10^{-3})$. (a)-(c) Mean estimates of P_m and P_p with corresponding 90% credible intervals, and the mean D_{KL} values, respectively, for the scrape assay for one, two and three observations. (d)-(f) Mean estimates of P_m and P_p with corresponding 90% credible intervals, and the mean D_{KL} values, respectively, for the wound assay for one, two and three observations. The mean D_{KL} values were calculated using Equation (3). The green bar corresponds to the D_{KL} value for P_p and the blue bar corresponds to the D_{KL} value for P_m. For all simulations $\tau = 1/24$ h, $N(0) = 100$, $M = 10^6$, $X = 36$, $Y = 27$, $\Delta = 25$ μm. For scrape assays, $Y_0 = 10$. For wound assays, $Y_{0,1} = Y_{0,2} = 5$. The crosses correspond to the mean values.

information is lost beyond that time. This suggests that interpreting experimental observations in a wound assay after the two cell fronts merge does not provide additional information about D and λ.

Currently, there is no explicit discussion in the experimental literature about the choice of the number of observations. Typically there is, at most, two observations made after the initial observation [1, 26, 30], which is due to the cost associated with capturing and interpreting experimental observations. Therefore, we restrict our analysis to consider, at most, three observations after the initial observation. We present the mean parameter estimates, and the mean of the corresponding 90% credible intervals, symmetric around the mode, that we obtain when we analyse one, two and three observations in Figures 6(a)-(b) and Figures 6(d)-(e), for the scrape and wound assays, respectively. While our estimates of P_m and P_p are sensitive to the number of observations, they are less sensitive compared to the choice of final observation time. To determine whether there is any benefit in capturing and interpreting additional experimental observations,

we calculate the mean D_{KL} value for P_m and P_p, for one, two and three observations. To obtain the mean D_{KL} value for one observation we consider the mean of four D_{KL} values. Each of these D_{KL} values is obtained using a combination of observation times that contains a single observation, that is, either 3 h, 6 h, 9 h or 12 h. We follow a similar process to obtain the mean D_{KL} values for two and three observations. For two and three observations we calculate the mean of the D_{KL} values obtained from all combinations of observation times that contain two and three observations, respectively. The mean D_{KL} values are given in Figures 6(c) and (f). In both assays, on average, there is a slight increase in the amount of information gained when we make two observations relative to when we make one observation. However, there is a much smaller amount of information gained when we make three observations, compared to two observations. The third observation does not provide a significant amount of additional information, even if we only compare combinations of observations that include $t = 12$ h. With this additional restriction, in the scrape assay, we obtain mean D_{KL} values of 7.95 and 8.05 for two and three observations, respectively. In the wound assay, we obtain mean D_{KL} values of 7.64 for both two and three observations. The lack of additional information obtained from interpreting three observations compared to two observations implies that there is likely to be further diminishing returns and we therefore recommend that making two observations is sufficient.

3.4. Choice of observation times: experimental data set

We repeat the process described in Section 3.3 for our experimental data set and calculate the mean model parameter estimates, and corresponding mean 90% credible intervals, for different final observation times. Again, we note that the wound assay was performed over 24 h and that we compare observation times after the same proportion of time has elapsed relative to the final time. For example, we compare an observation at 6 h in the scrape assay with an observation at 12 h in the wound assay. We present the mean model parameter estimates and 90% credible intervals in Figures 7(a)-(b) and Figures 7(d)-(e), for the scrape and wound assays, respectively. Similar to the synthetic results, we observe that the estimates of D are more sensitive to the choice of final observation time in the wound assay. Additionally, estimates of λ are more sensitive to the choice of final observation time in the wound assay, a trend that is not observed in the synthetic data set. Interestingly, while the estimates of λ are more sensitive in the wound assay, the D_{KL} values corresponding to λ, represented by the green bar in Figures 7(c) and (f), are higher for the wound than the scrape assay. We attribute this to the additional number of cells present in the wound assay, which may influence the information gained but not the relationship between λ and the final observation time. The D_{KL} value for the scrape assay, given in Figure 7(c), increases with the final observation time. Conversely, the D_{KL} value for the wound assay, given in Figure 7(f), does not increase significantly after a final observation time of 12 h. We observe that the composition of the D_{KL} value for the wound assay changes with the final observation time; as the final observation time increases, the D_{KL} value for D decreases and the D_{KL} value for λ increases, while the sum of the two D_{KL} values is approximately constant. This result

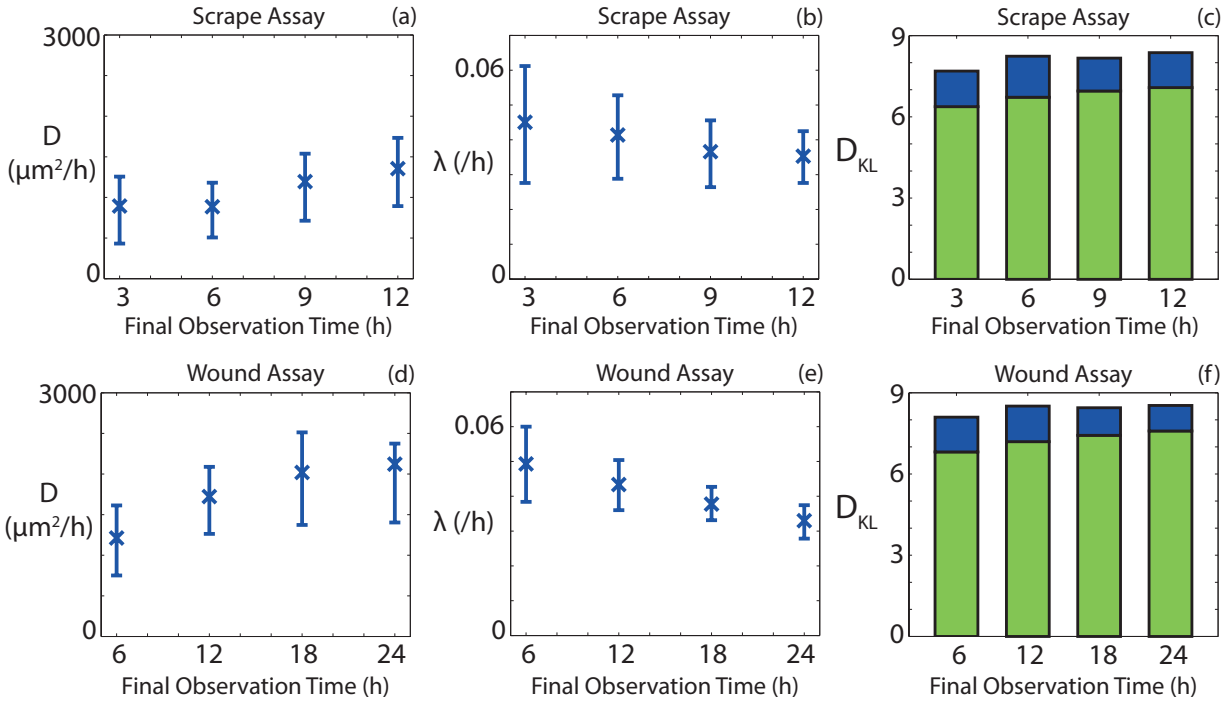

Figure 7: Results obtained from the parameter inference approach applied to the experimental data set. (a)-(c) Mean estimates of P_m and P_p with corresponding 90% credible intervals, and the mean D_{KL} values, respectively, for the scrape assay for a final observation time of 3 h, 6 h, 9 h and 12 h. (d)-(f) Mean estimates of P_m and P_p with corresponding 90% credible intervals, and the mean D_{KL} values, respectively, for the wound assay for a final observation time of 3 h, 6 h, 9 h and 12 h. The mean D_{KL} values were calculated using Equation (3). The green bar corresponds to the D_{KL} value for λ and the blue bar corresponds to the D_{KL} value for D. For all simulations $\tau = 1/24$ h, $M = 10^6$, $X = 36$, $Y = 49$, $\Delta = 25$ μm. For scrape assays, $N(0) = 155$, $Y_0 = 10$. For wound assays, $N(0) = 226$, $Y_{0,1} = 7, Y_{0,2} = 9$.

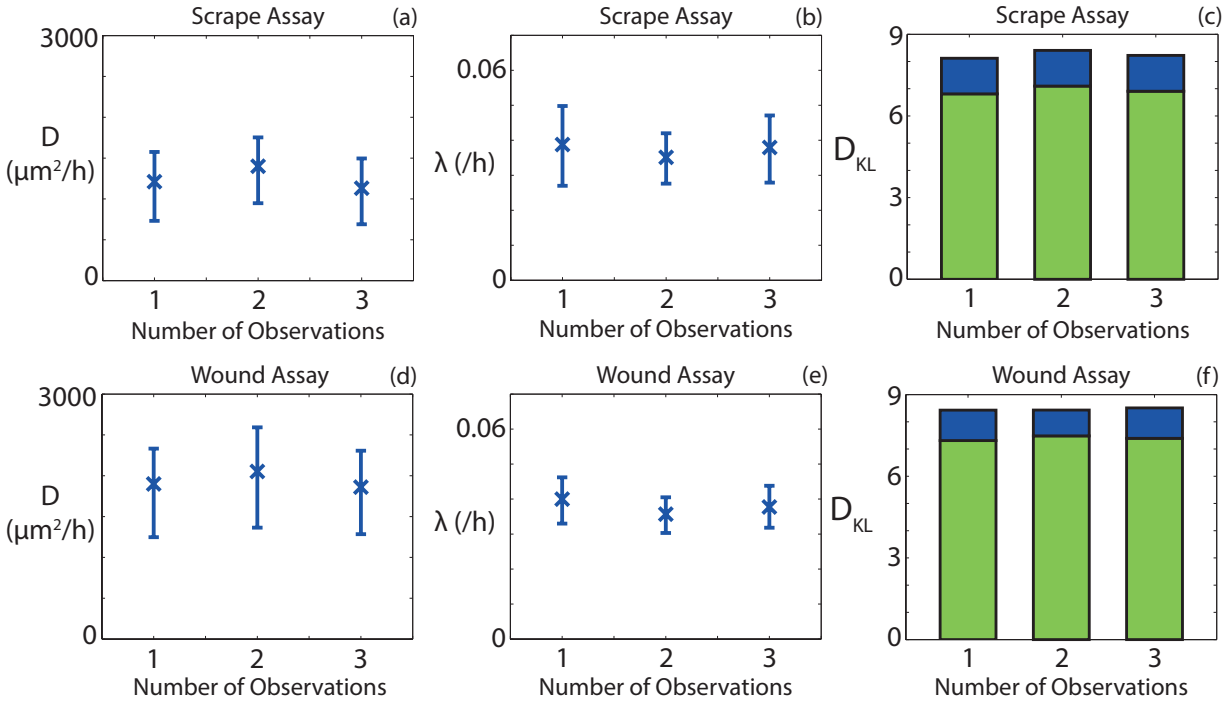

Figure 8: Results obtained from the parameter inference approach applied to the experimental data set. (a)-(c) Mean estimates of P_m and P_p with corresponding 90% credible intervals, and the mean D_{KL} values, respectively, for the scrape assay for one, two and three observations. (d)-(f) Mean estimates of P_m and P_p with corresponding 90% credible intervals, and the mean D_{KL} values, respectively, for the wound assay for one, two and three observations. The mean D_{KL} values were calculated using Equation (3). The green bar corresponds to the D_{KL} value for λ and the blue bar corresponds to the D_{KL} value for D. For all simulations $\tau = 1/24$ h, $M = 10^6$, $X = 36$, $Y = 49$, $\Delta = 25$ μm. For scrape assays, $N(0) = 155$, $Y_0 = 10$. For wound assays, $N(0) = 226$, $Y_{0,1} = 7, Y_{0,2} = 9$.

is consistent with the synthetic wound assay, where we observed that information about D is lost when the two cell fronts began to interact.

We now examine the influence of the number of observations on our estimates of D and λ and the corresponding D_{KL} values. The mean model parameter estimates for all combinations of observation times, for one, two and three observations are presented, with the corresponding mean 90% credible interval for D and λ, in Figures 8(a)-(b) and Figures 8(d)-(e) for the scrape and wound assays, respectively. For both model parameters and assays, the parameter estimates are less sensitive to the number of observations than to the final observation time, which is consistent with the synthetic results. It is instructive to consider whether the number of observations influences D_{KL}, to provide guidance about the number of experimental observations that ought to be captured. We present the D_{KL} values for one, two and three observations for the scrape and wound assays in Figures 8(c) and (f), respectively. Similar to the synthetic results for the data set in Section 3.3, there is no significant increase in information gained between two and three

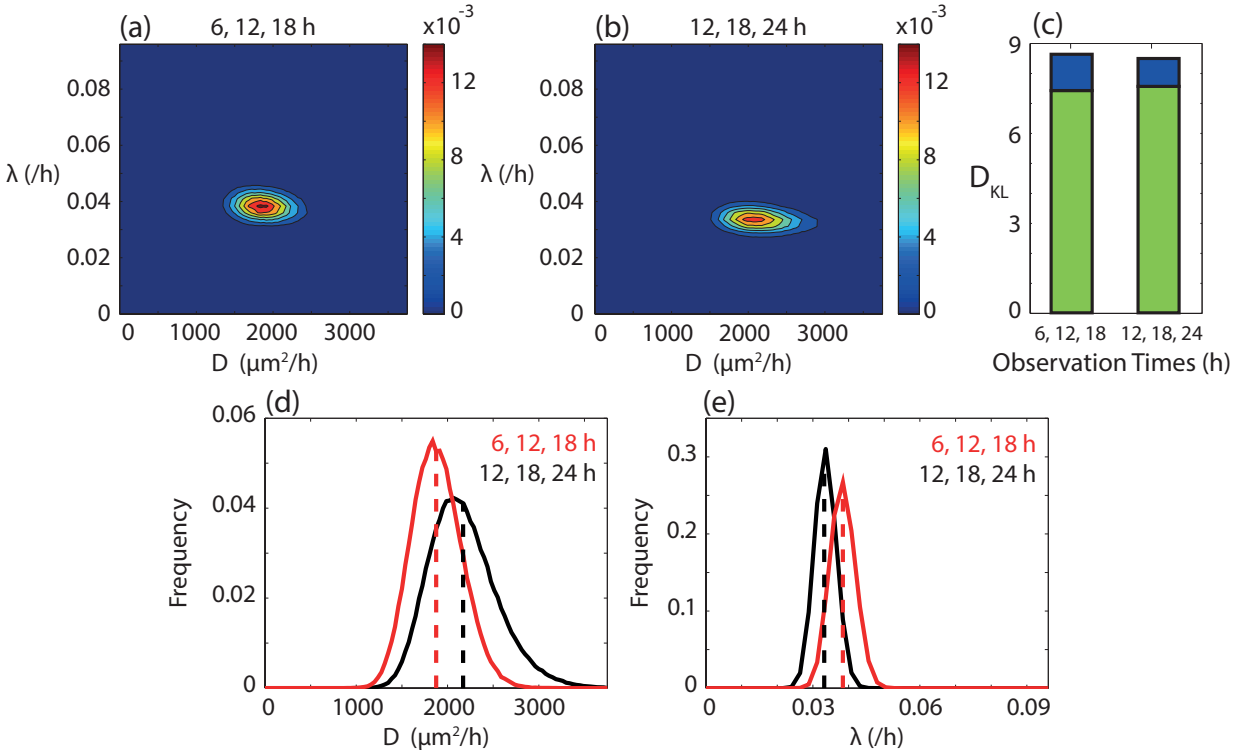

Figure 9: Approximate posterior distributions corresponding to different combinations of observation times for the wound assay experimental data set. (a)-(b) Approximate posterior distribution using observations at (a) 6, 12 and 18 h and (b) 12, 18 and 24 h. (c) Mean D_{KL} values for 6, 12 and 18, and for 12, 18 and 24 h. The mean D_{KL} values were calculated using Equation (3). The green bar corresponds to the D_{KL} value for λ and the blue bar corresponds to the D_{KL} value for D. (d)-(e) Corresponding marginal distributions for (d) D and (e) λ. Red curves are obtained from observations at 6, 12 and 18 h, while the black curves are obtained from observations at 12, 18 and 24 h. Dashed lines correspond to mean parameter estimates. For all simulations $\tau = 1/24$ h, $M = 10^6$, $X = 36$, $Y = 49$, $N(0) = 226$, $Y_{0,1} = 7, Y_{0,2} = 9$, $\Delta = 25$ μm.

observations, implying that capturing and interpreting additional experimental observations is unnecessary. Given that the interpretation of experimental observations is both time-consuming and expensive, this result provides useful guidance about the number of experimental observations required to estimate D and λ.

For all data sets we observe that it is possible to obtain consistent D_{KL} values with different combinations of observation times, suggesting that various experimental designs are equally informative. However, it is also important to consider the ratio of the D_{KL} values associated with the marginal distributions of P_m and P_p. To illustrate this, we present the approximate posterior distributions of D and λ for the experimental wound assay data set using the combinations of observation times at 6, 12, 18 h, and 12, 18, 24 h in Figures 9(a)-(b), respectively. The D_{KL} values, presented in Figure 9(c), for the two posterior distributions are similar: 8.63 and 8.50, respectively, suggesting that both are approximately equally informative. However, if we consider the marginal distributions, we find that the 6, 12, 18 h design results in approximately 30% extra information about D compared to the 12, 18, 24 h design, while retaining 97% of the information about

λ. The marginal distributions in Figures 9(d)-(e) illustrate the relative information gain for the two designs. We observe that the marginal distribution for D varies significantly, in particular the width of support of the distribution is very different, while the marginal distributions for λ are relatively consistent. The change in distribution for D suggests that the ratio between marginal D_{KL} values can be used to distinguish between posterior distributions that have similar D_{KL} values.

4. Summary of results and recommendations

Our results provide guidance about experimental design choices for scratch assays. For both synthetic and experimental data sets we observe that the scrape assay provides estimates of D and λ that are less sensitive to the choice of observation times. For the synthetic data set, where D and λ are known in advance, the scrape assay provides more robust estimates of D and λ. With regard to the information gained about D and λ, defined using the Kullback-Leibler divergence, the scrape assay is superior for the synthetic data set. Conversely, for the experimental data set, the wound assay provides more information about the model parameters than the scrape assay. However, if we consider the D_{KL} values for the marginal distribution of D and λ, we see that the additional information gained in the wound assay is primarily associated with λ. This result is intuitive for the experimental data set, as initially there are significantly more cells in the wound assay than in the scrape assay, in contrast with the synthetic data set where the initial number of cells is the same for both assays. We found that the increase in the initial number of cells results in an increase in computational time of approximately one order of magnitude between the scrape assay and the wound assay. The majority of combinations of observation times for the scrape assay lead to more information about D than the corresponding combinations of observation times for the wound assay. As the D_{KL} values associated with the marginal distribution of D are significantly lower than those associated with the marginal distribution of λ, an increase in information about D is more significant than an equivalent absolute increase in information about λ. Therefore, since the scrape assay provides more robust estimates of D and λ, is less sensitive to the choice of combination of observation times, and is more computationally efficient, we recommend that scrape assays, instead of wound assays, ought to be used to estimate D and λ. We note that these recommendations are based upon experimental observations for a mesenchymal (non-adhesive) cell population and that our recommendations may not be valid for cell populations that involve significant cell-to-cell adhesion.

The uncertainty in our estimates of λ is sensitive to the data obtained at the final observation time. It is intuitive to consider the estimate of λ obtained from a combination of experimental observations that include the latest final observation time, as it is difficult to characterise λ for an experimental time that is significantly less than the cell doubling time, which is approximately 24 h [16]. For the scrape assay, using

both experimental and synthetic data sets, we observe that using a final observation time corresponding to time taken for the cell front to cross the experimental field of view provides the most information about D and λ. The choice of the number of observations captured and interpreted affects both the cost and amount of time required to analyse an experiment. Therefore, there is a considerable advantage in minimising the number of observations. We note that the main cost of our approach is associated with the interpretation, rather than the capture, of the experimental images. Therefore, if there is no prior estimate of D, which provides guidance about the final experimental time, images can be captured until the cell front has crossed the experimental field of view. The choice of which images to interpret can then be made after the experiment is performed and the final observation time is determined. For both assays and data sets, we observe that there is, at best, a small increase in information gained by interpreting three experimental observations compared to two. To minimise the expense associated with interpreting experiments, we recommend that two experimental observations are captured, after the initial observation. The time when the first observation is captured, after the initial observation, does not significantly influence the information obtained, compared to the final observation time. As such, we do not provide a recommendation for the time when the first observation should be captured.

5. Discussion and conclusions

Scratch assays are widely used to observe collective cell spreading and to examine the influence of potential drugs on the rates of cell motility and proliferation [11, 19, 20, 41]. However, the experimental design of scratch assays reported in the literature varies considerably [1, 5, 16, 17, 25, 26, 30]. The number of experimental observations, the timing at which the observations are captured, and the type of scratch assay are all technically straightforward to vary but there is no explicit discussion in the literature about the influence of these design choices. To the best of our knowledge, there is no biological justification associated with the choice of assay type. Instead, this choice appears to be made according to personal preference. Mathematical models that can be used to estimate D and λ have been presented previously, but these previous applications have not considered the influence of varying experimental designs [5, 16, 17, 28, 40]. To address this limitation, we quantify the information gained about the D and λ, depending on whether a scrape or wound assay is performed. We also investigate the amount of information gained depending on how many experimental observations are captured, and the timing of these observations. To interpret the experimental observations we use an ABC method which provides an approximate bivariate posterior distribution of D and λ [17]. This allows us to quantify the amount of information gained about the model parameters, D and λ, thereby providing guidance about the influence of the experimental design. By identifying experimental designs that allow for more robust parameter estimation, we can make objective recommendations about

the number of experimental observations required and, subsequently, reduce the time and cost requirements.

We find that a scrape assay, with just one cell front, provides more robust estimates of the random motility, D, and the cell proliferation rate, λ, is more computationally efficient, requires less time to locate cell positions, and provides more information about D, without sacrificing too much information about λ, compared to the wound assay. Therefore, if the aim is to estimate D and λ, we recommend that scrape assays, and not wound assays, be performed. We find that most information about D and λ is obtained when the final observation time corresponds to the amount of time taken for the front to migrate across the experimental field of view. We also find there is limited benefit to capturing three observations, compared to two.

The work presented here could be extended in several ways. We note that our experimental analysis is relevant for a mesenchymal cell population and that the influence of cell-to-cell or cell-to-substrate adhesion in epithelial cell populations may affect our recommendations. In our mathematical model, we make the standard assumption that both D and λ are constant [16, 17, 33, 34], However, from the results presented in Figure 7, we observe that D appears to increase with time. It is possible that the cells are disrupted by the initial scratch or the addition of fresh medium immediately after the scratch is performed. We do not make any suggestion about the putative form of any model parameters that may depend on time or local cell density. It would be instructive to consider an extension to our discrete mathematical model with parameters that are not constant [8, 13] and, subsequently, to investigate whether ABC can result in robust model parameter estimates for a more complicated mathematical model. Such a model may require a different choice of summary statistic and we could employ a semi-automatic approach to determine an appropriate summary statistic [10]. A similar investigation of potential summary statistics for a model that includes parameters that are sensitive to chemical gradients could be performed. However, introducing chemotaxis into the mathematical model increases both the complexity of the model and the number of unknown model parameters. For example, a chemotaxis model would include the diffusivity of the attractant, the production rate of the attractant, the decay rate of the attractant, as well as the parameters governing the chemotactic sensitivity function [18]. We therefore leave this for future work. Alternatively, we could apply the approach outlined in this work to different types of *in vitro* experiments, such as two-dimensional barrier assays or three-dimensional spheroid assays, to quantify the impact of experimental design choices. We make two approximations to compare the cell positions in the experimental images to the mathematical model. First, we assume that cells are incompressible, uniformly-sized disks and, second, we map the cell positions on to a regular lattice with lattice spacing equivalent to the average cell diameter [34]. It would be instructive to relax these assumptions by considering cells that are able to deform or by considering a lattice-free mathematical model. However, both of these approaches would significantly increase the com-

plexity of the mathematical model. Subsequently, the time required to perform the ABC algorithm would become intractable and, as such, we leave this extension for a future study.

Acknowledgements: This work is supported by the Cooperative Research Centre for Wound Management Innovation and the Australian Research Council (FT130100148, FT130100254). We appreciate the support provided by the High Performance Computing Centre at QUT. We thank the three referees for their helpful comments.

[1] K. Aichele, M. Bubel, G. Deubel, T. Pohlemann, and M. Oberringer. Bromelain down-regulates myofibroblast differentiation in an in vitro wound healing assay. *Naunyn-Schmiedeberg's Archives of Pharmacology*, 386:853–763, 2013.

[2] M. A. Beaumont, W. Zhang, and D. J. Balding. Approximate Bayesian computation in population genetics. *Genetics*, 162(4):2025–2035, 2002.

[3] B. J. Binder and M. J. Simpson. Quantifying spatial structure in experimental observations and agent-based simulations using pair-correlation functions. *Physical Review E*, 88(2):022705, 2013.

[4] K. P. Burnham and D. R. Anderson. *Model selection and multimodel inference: a practical information-theoretic approach*. Springer, 2002.

[5] A. Q. Cai, K. A. Landman, and B. D. Hughes. Multi-scale modeling of a wound-healing cell migration assay. *Journal of Theoretical Biology*, 245(3):576–594, 2007.

[6] K. Chaloner and I. Verdinelli. Bayesian experimental design: A review. *Statistical Science*, pages 273–304, 1995.

[7] E. A. Codling, M. J. Plank, and S. Benhamou. Random walk models in biology. *Journal of the Royal Society Interface*, 5(25):813–834, 2008.

[8] C. W. Curtis and D. M. Bortz. Propagation of fronts in the Fisher-Kolmogorov equation with spatially varying diffusion. *Physical Review E*, 86(6):066108, 2012.

[9] G. B. Ermentrout and L. Edelstein-Keshet. Cellular automata approaches to biological modeling. *Journal of Theoretical Biology*, 160(1):97–133, 1993.

[10] P. Fearnhead and D. Prangle. Constructing summary statistics for approximate bayesian computation: semi-automatic approximate bayesian computation. *Journal of the Royal Statistical Society: Series B*, 74(3):419–474, 2012.

[11] D. A. Fishman, Y. Liu, S. M. Ellerbroek, and M. S. Stack. Lysophosphatidic acid promotes matrix metalloproteinase (MMP) activation and MMP-dependent invasion in ovarian cancer cells. *Cancer Research*, 61(7):3194–3199, 2001.

[12] A. Habbal, H. Barelli, and G. Malandain. Assessing the ability of the 2D Fisher–KPP equation to model cell-sheet wound closure. *Mathematical Biosciences*, 252:45–59, 2014.

[13] J. F. Hammond and D. M. Bortz. Analytical solutions to Fishers equation with time-variable coefficients. *Applied Mathematics and Computation*, 218(6):2497–2508, 2011.

[14] W. Jin, E. T. Shah, C. J. Penington, S. W. McCue, L. K. Chopin, and M. J. Simpson. Reproducibility of scratch assays is affected by the initial degree of confluence: Experiments, modelling and model selection. *Journal of Theoretical Biology*, 390:136–145, 2016.

[15] S. T. Johnston, E. T. Shah, L. K. Chopin, D. S. McElwain, and M. J. Simpson. Estimating cell diffusivity and cell proliferation rate by interpreting IncuCyte ZOOM assay data using the Fisher-Kolmogorov model. *BMC Systems Biology*, 9(1):38, 2015.

[16] S. T. Johnston, M. J. Simpson, and D. L. S. McElwain. How much information can be obtained from tracking the position of the leading edge in a scratch assay? *Journal of the Royal Society Interface*, 11(97):20140325, 2014.

[17] S. T. Johnston, M. J. Simpson, D. L. S. McElwain, B. J. Binder, and J. V. Ross. Interpreting scratch assays using pair density dynamics and approximate Bayesian computation. *Open Biology*, 4(9):140097, 2014.

[18] E. F. Keller and L. A. Segel. Model for chemotaxis. *Journal of Theoretical Biology*, 30(2):225–234, 1971.

[19] D. A. Knecht, R. A. LaFleur, A. W. Kahsai, C. E. Argueta, A. B. Beshir, and G. Fenteany. Cucurbitacin I inhibits cell motility by indirectly interfering with actin dynamics. *PLOS ONE*, 5(11):e14039, 2010.

[20] R. Landesberg, M. Cozin, S. Cremers, V. Woo, S. Kousteni, S. Sinha, L. Garrett-Sinha, and S. Raghavan. Inhibition of oral mucosal cell wound healing by bisphosphonates. *Journal of Oral and Maxillofacial Surgery*, 66(5):839–847, 2008.

[21] C.-C. Liang, A. Y. Park, and J.-L. Guan. In vitro scratch assay: a convenient and inexpensive method for analysis of cell migration in vitro. *Nature Protocols*, 2(2):329–333, 2007.

[22] R. Lukeman, Y.-X. Li, and L. Edelstein-Keshet. Inferring individual rules from collective behavior. *Proceedings of the National Academy of Sciences*, 107(28):12576–12580, 2010.

[23] P. K. Maini, D. L. S. McElwain, and D. Leavesley. Travelling waves in a wound healing assay. *Applied Mathematics Letters*, 17(5):575–580, 2004.

[24] P. Marjoram, J. Molitor, V. Plagnol, and S. Tavaré. Markov chain Monte Carlo without likelihoods. *Proceedings of the National Academy of Sciences*, 100(26):15324–15328, 2003.

[25] F. M. Meier, K. W. Frommer, M. A. Peters, F. Brentano, S. Lefèvre, D. Schröder, D. Kyburz, J. Steinmeyer, S. Rehart, S. Gay, et al. Visfatin/pre-b-cell colony-enhancing factor (PBEF), a proinflammatory and cell motility-changing factor in

rheumatoid arthritis. *Journal of Biological Chemistry*, 287(34):28378–28385, 2012.

[26] V. Rausch, L. Liu, A. Apel, T. Rettig, J. Gladkich, S. Labsch, G. Kallifatidis, A. Kaczorowski, A. Groth, W. Gross, et al. Autophagy mediates survival of pancreatic tumour-initiating cells in a hypoxic microenvironment. *The Journal of Pathology*, 227(3):325–335, 2012.

[27] R. Riahi, Y. Yang, D. D. Zhang, and P. K. Wong. Advances in wound-healing assays for probing collective cell migration. *Journal of Laboratory Automation*, 17(1):59–65, 2012.

[28] B. G. Sengers, C. P. Please, and R. O. Oreffo. Experimental characterization and computational modelling of two-dimensional cell spreading for skeletal regeneration. *Journal of the Royal Society Interface*, 4(17):1107–1117, 2007.

[29] A. Shatkin, E. Reich, R. Franklin, and E.-L. Tatum. Effect of mitomycin-c on mammalian cells in culture. *Biochimica et Biophysica Acta*, 55(3):277–289, 1962.

[30] A. Shibata, E. Tanabe, S. Inoue, M. Kitayoshi, S. Okimoto, M. Hirane, M. Araki, N. Fukushima, and T. Tsujiuchi. Hydrogen peroxide stimulates cell motile activity through lpa receptor-3 in liver epithelial wb-f344 cells. *Biochemical and Biophysical Research Communications*, 433:317–321, 2013.

[31] M. J. Simpson, K. A. Landman, and B. D. Hughes. Multi-species simple exclusion processes. *Physica A: Statistical Mechanics and its Applications*, 388(4):399–406, 2009.

[32] M. J. Simpson, K. A. Landman, and B. D. Hughes. Cell invasion with proliferation mechanisms motivated by time-lapse data. *Physica A: Statistical Mechanics and its Applications*, 389(18):3779–3790, 2010.

[33] M. J. Simpson, K. A. Landman, B. D. Hughes, and A. E. Fernando. A model for mesoscale patterns in motile populations. *Physica A: Statistical Mechanics and its Applications*, 389(7):1412–1424, 2010.

[34] M. J. Simpson, K. K. Treloar, B. J. Binder, P. Haridas, K. J. Manton, D. I. Leavesley, D. L. S. McElwain, and R. E. Baker. Quantifying the roles of cell motility and cell proliferation in a circular barrier assay. *Journal of the Royal Society Interface*, 10(82):20130007, 2013.

[35] S. A. Sisson, Y. Fan, and M. M. Tanaka. Sequential Monte Carlo without likelihoods. *Proceedings of the National Academy of Sciences*, 104(6):1760–1765, 2007.

[36] G. J. Todaro and H. Green. Quantitative studies of the growth of mouse embryo cells in culture and their development into established lines. *The Journal of Cell Biology*, 17(2):299–313, 1963.

[37] T. Toni, D. Welch, N. Strelkowa, A. Ipsen, and M. P. Stumpf. Approximate Bayesian computation scheme for parameter inference and model selection in dynamical systems. *Journal of the Royal Society Interface*, 6(31):187–202, 2009.

[38] K. K. Treloar, M. J. Simpson, P. Haridas, K. J. Manton, D. I. Leavesley, D. L. S. McElwain, and R. E. Baker. Multiple types of data are required to identify the mechanisms influencing the spatial expansion of melanoma cell colonies. *BMC Systems Biology*, 7(1):137, 2013.

[39] K. K. Treloar, M. J. Simpson, D. S. McElwain, and R. E. Baker. Are in vitro estimates of cell diffusivity and cell proliferation rate sensitive to assay geometry? *Journal of Theoretical Biology*, 356:71–84, 2014.

[40] A. Tremel, A. Cai, N. Tirtaatmadja, B. D. Hughes, G. W. Stevens, K. A. Landman, and A. J. O'Connor. Cell migration and proliferation during monolayer formation and wound healing. *Chemical Engineering Science*, 64(2):247–253, 2009.

[41] Z. Upton, H. J. Wallace, G. K. Shooter, D. R. van Lonkhuyzen, S. Yeoh-Ellerton, E. A. Rayment, J. M. Fleming, D. Broszczak, D. Queen, R. G. Sibbald, et al. Human pilot studies reveal the potential of a vitronectin: growth factor complex as a treatment for chronic wounds. *International Wound Journal*, 8(5):522–532, 2011.

[42] B. N. Vo, C. C. Drovandi, A. N. Pettitt, and M. J. Simpson. Quantifying uncertainty in parameter estimates for stochastic models of collective cell spreading using approximate Bayesian computation. *Mathematical Biosciences*, 263:133–142, 2015.